

Forming silicon carbon nitride crystals and silicon carbon nitride nanotubes by microwave plasma-enhanced chemical vapor deposition

Hui Lin Chang, Chih Ming Hsu, and Cheng Tzu Kuo

Citation: [Applied Physics Letters](#) **80**, 4638 (2002); doi: 10.1063/1.1487925

View online: <http://dx.doi.org/10.1063/1.1487925>

View Table of Contents: <http://scitation.aip.org/content/aip/journal/apl/80/24?ver=pdfcov>

Published by the [AIP Publishing](#)

Articles you may be interested in

[Carbon nanowalls grown by microwave plasma enhanced chemical vapor deposition during the carbonization of polyacrylonitrile fibers](#)

J. Appl. Phys. **113**, 024313 (2013); 10.1063/1.4774218

[Role of plasma activation in kinetics of carbon nanotube growth in plasma-enhanced chemical vapor deposition](#)

J. Appl. Phys. **111**, 074307 (2012); 10.1063/1.3699310

[Growth of aligned carbon nanotubes on carbon microfibers by dc plasma-enhanced chemical vapor deposition](#)

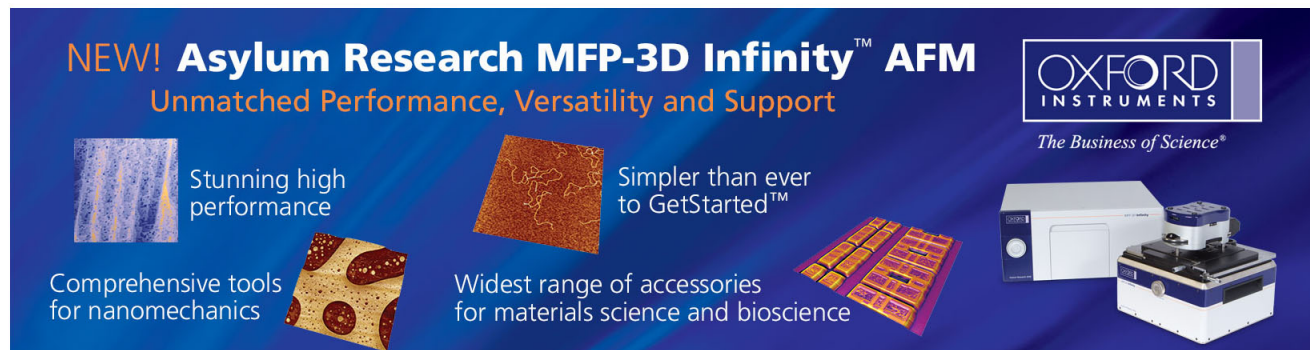
Appl. Phys. Lett. **88**, 033103 (2006); 10.1063/1.2166472

[Growing carbon nanotubes by microwave plasma-enhanced chemical vapor deposition](#)

Appl. Phys. Lett. **72**, 3437 (1998); 10.1063/1.121658

[Structure of fluorine-doped silicon oxide films deposited by plasma-enhanced chemical vapor deposition](#)

J. Vac. Sci. Technol. A **15**, 2908 (1997); 10.1116/1.580884



NEW! Asylum Research MFP-3D Infinity™ AFM
Unmatched Performance, Versatility and Support

OXFORD INSTRUMENTS
The Business of Science®

Stunning high performance
Simpler than ever to GetStarted™
Comprehensive tools for nanomechanics
Widest range of accessories for materials science and bioscience

The advertisement features four images: a textured surface, a brown surface with a network of lines, a grid of small rectangular samples, and the MFP-3D Infinity AFM instrument.

Forming silicon carbon nitride crystals and silicon carbon nitride nanotubes by microwave plasma-enhanced chemical vapor deposition

Hui Lin Chang,^{a)} Chih Ming Hsu, and Cheng Tzu Kuo

Department of Material Science and Engineering, National Chiao Tung University, Hsinchu, Taiwan

(Received 4 March 2002; accepted for publication 24 April 2002)

Catalyst-assisted silicon carbon nitride (SiCN) nanotubes and SiCN crystals are prepared. The SiCN nanotubes and SiCN crystals are formed by gaseous sources of $\text{CH}_4/\text{N}_2/\text{H}_2$ and CH_4/N_2 , respectively, and using solid Si columns arranged symmetrically around the specimen as additional Si sources. The formation of the tubular structure is related to the ambient of process that includes H_2 gas, which is considered to delay the action of the so-called catalyst poisons and keep the tube end open during growth. Analysis shows that the SiCN crystals exhibit tetragonal or hexagonal shapes with sizes of about several microns, and multibonding structures. In contrast, the SiCN tubes are randomly orientated with various diameters, and graphitelike structure. The growth mechanisms of SiCN crystals and SiCN nanotubes are discussed. © 2002 American Institute of Physics. [DOI: 10.1063/1.1487925]

Liu and Cohen in 1989¹ predicted that covalently bonded $\beta\text{-C}_3\text{N}_4$ could be harder than the diamond, which has stimulated much interest in synthesizing C_3N_4 and silicon carbon nitride SiCN crystals.²⁻⁴ These superhard materials are expected to exhibit excellent properties such as thermal conductivity, chemical inertness, and a wide band gap.^{5,6} The identification of the structure of C_{60} by Kroto *et al.* in 1985⁷ and of carbon nanotube (CNTs) by Iijima in 1991⁸ were important events for the scientific community. Those discoveries not only led to the development of nanotechnology but also to fundamental research into nanometer sized materials. Doped C_{60} with alkali metals (M_3C_{60}) can be a superconductor in various applications.⁹ Besides, CNTs have been shown to have a great potential in applications of scanning probe,¹⁰ supercapacitors,¹¹ hydrogen storage,¹² and field-emission display.¹³ Nanotubes, except for well-known CNTs, other nanotubes (NTs) such as WS_2 , MoS_2 , BN, BCN, and V_2O_5 have been recently studied, and have been found to possess characteristics other than CNTs.¹⁴⁻¹⁸ Spherical nanostructures of carbon nitride were also studied by depositing it on a porous substrate.¹⁹ Consequently, discovering new materials with nanotube or nanofiber structures is also an interesting subject. In this letter, we adopt a single tool to synthesize SiCN crystals and SiCN nanotubes, and the synthesis conditions for these two structures are linked. Mechanisms of formation are proposed.

SiCN crystals and SiCN nanotubes were synthesized on Co (100 nm) coated Si wafers using a microwave plasma chemical vapor deposition system, where Co film was formed by physical vapor deposition. The additional Si sources were inserted into specimen holder symmetrically around the specimen. Figure 1 schematically shows process conditions and the positions of Si columns relative to the sample. The synthesis steps were as follows. (1) H_2 reduction for 10 min at 5 Torr, and a microwave power of 500 W, followed by (2) that introduction of CH_4/N_2 or $\text{CH}_4/\text{N}_2/\text{H}_2$

process gases, in a ratio of 10/100 sccm or 10/100/50 sccm, at a deposition pressure of 12 Torr, respectively, and a microwave power of 800 W, for 4 h. Scanning electron microscopy (SEM) was employed to examine the film morphologies. The SiCN film compositions and bonding structures were determined by x-ray photoelectron spectroscopy (XPS). High-resolution transmission electron microscopy (HRTEM) was used to characterize microstructures of the nanotubes, and electron energy loss spectroscopy (EELS) equipped with TEM was used to determine the bonding structures of NTs.

SiCN crystals and SiCN/nanotubes were synthesized with the same process parameters except the gaseous source of the former was a mixtures of CH_4/N_2 gases and that of the latter was at $\text{CH}_4/\text{N}_2/\text{H}_2$ gases. Figure 2(a) shows the typical SiCN crystal morphologies, which are similar to those in our previous work,²⁻⁴ in which tetragonal or hexagonal facet crystals of μm size were observed. Meanwhile, Fig. 2 (b) shows the tubularlike structures of SiCN indicating the random orientations and various tube diameters. The effect of the H_2 gas on either the SiCN crystal or the SiCN tube formations is interesting and can be interpreted in the following two ways. The first is that hydrogen removes the graphite overlayer coated on the surface of catalyst particle.

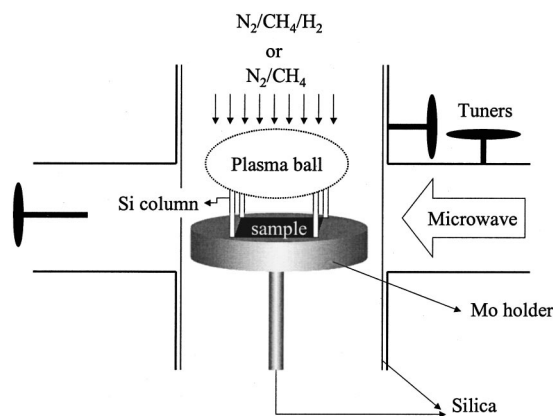


FIG. 1. Relative positions between Si columns and the sample in a reactor.

^{a)}Electronic mail: gladies@mail.mayju.com.tw

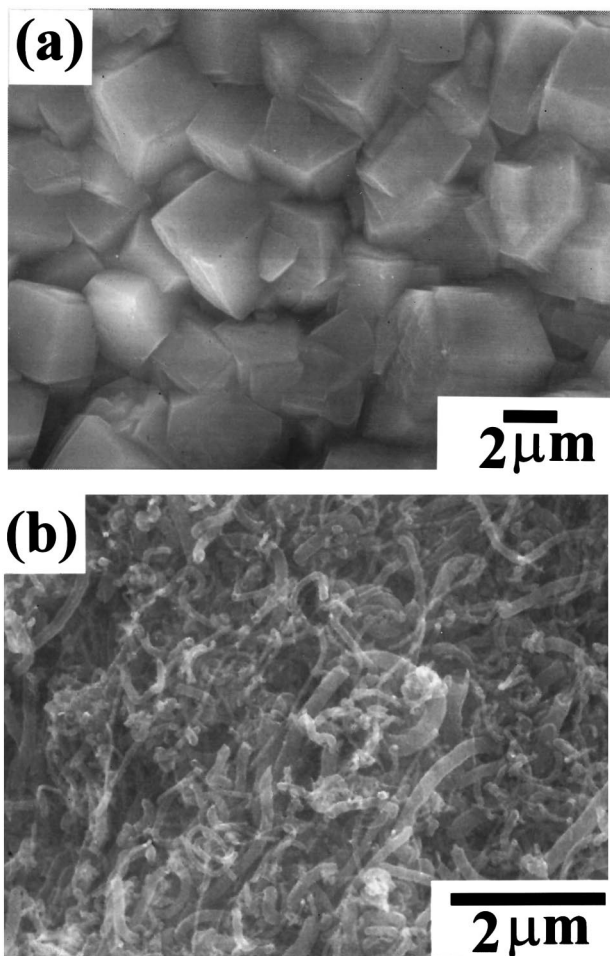


FIG. 2. SEM morphologies of (a) SiCN crystals and (b) SiCN nanotubes formed using Co catalyst film.

This overlayer hinders the desorbing and dissolving of carbon atoms in the catalyst particles, equivalent to blocking the catalytic action of the transition metal.²⁰ Accordingly, the “clean” surface exposed by H₂ etching allows the succeeding C atoms to dissolve in the catalyst, and then to precipitate a graphitelike structure around the catalyst particle. Tubularlike structures are thus formed. The second interpretation is that H₂ gas promotes the graphitelike structure formation. Reconstruction of the end of the tube by H₂ atoms can prolong the tube “opening,”²¹ since the H₂ atoms bond to the exposed dangling bonds of carbon. Here, the role of the catalyst in forming SiCN tubes is similar to that of the proposed models of Baker *et al.*,²² Oberlin *et al.*,²³ and Tibbetts,²⁴ who employed the concepts of the vapor–liquid–solid model.²⁵ The tube grows by precipitation of graphite sheets from a supersaturated catalytic droplet. The formation of curved graphite basal plane is energetically favorable, and so the tubular structure is formed. The base growth model is suggested to dominate the growth of SiCN nanotubes because the catalyst particle at the tip of the tube was not observed in the SEM top view investigation. In comparison, the catalytic functions of the process ambient without H₂ gas differ from those with H₂ gas. The catalysts are suggested to provide nucleation sites for SiCN crystal nucleation, and effectively reduce the energy of formation at the initial stage. As the growing film covers the catalytic particle, the catalytic function is lost. The film morphologies depend on the

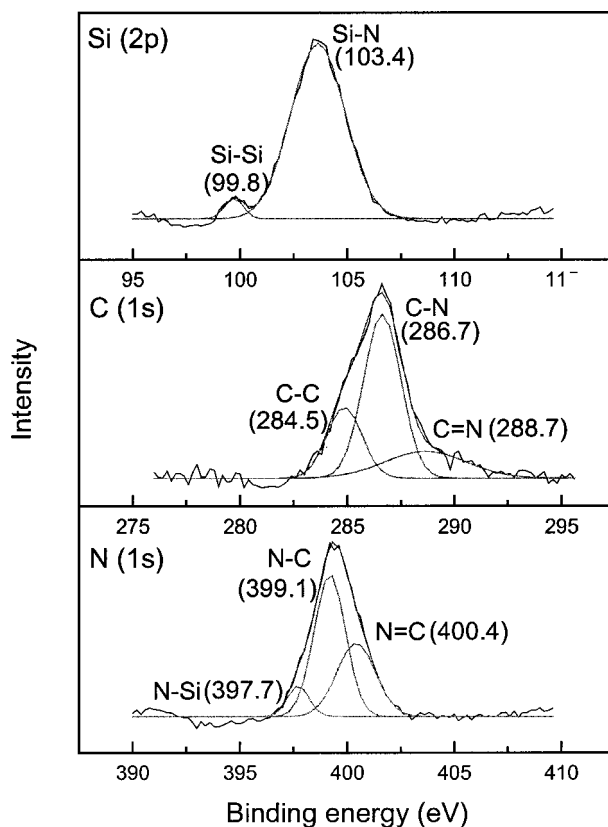


FIG. 3. XPS spectrum of SiCN crystals (a) Si (2p) core level, (b) C (1s) core level, and (c) N (1s) core level.

buffer layer and substrate treatment according to our previous study,² because the extra buffer layer, such as Fe or Co, can markedly increase the film deposition rate, which is proven by the higher deposition rate when a catalyst is added (2.5 μm/h) than that when none is added (1 μm/h).

The XPS and EELS were selected, to identify the bonding structure of SiCN crystal and SiCN NT, respectively. Figure 3 shows high resolution XPS scans of core levels of Si (2p), C (1s), and N (1s). These spectra deconvoluted by Gaussian fitting consist of subpeaks. The deconvoluted peaks shows that the bonding of Si(2p)—Si, Si(2p)—N, C(1s)—C, C(1s)—N, C(1s)=N, N(1s)—Si, N(1s)—C, and N(1s)=C are at 99.8 eV, 103.4 eV, 284.5 eV, 286.7 eV,

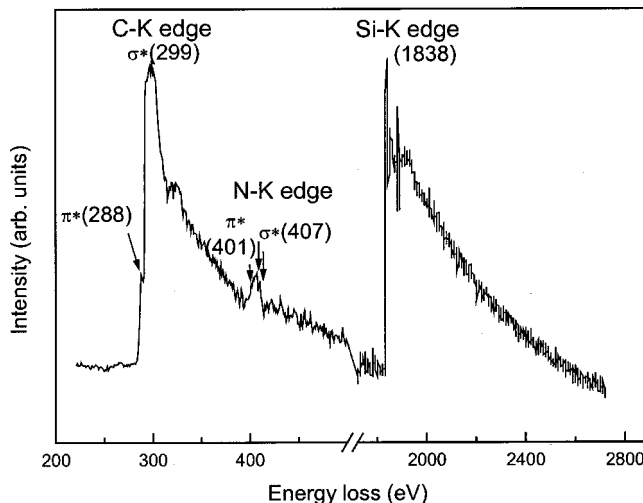


FIG. 4. EELS spectrum of SiCN nanotube recorded from the tube walls.

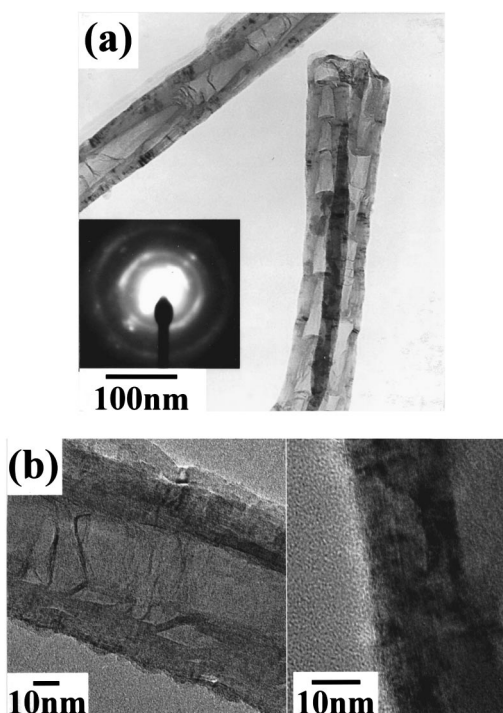


FIG. 5. TEM images of SiCN nanotube at (a) low magnification with the corresponding electron diffraction pattern (b) high magnification.

288.7 eV, 397.7 eV, 399.1 eV, and 400.4 eV, respectively. In conclusion, the SiCN crystals are multibonding structures. Figure 4 shows the EELS spectrum of SiCN nanotubes. The K -shell ionizations of C, N, and Si occur at 288 eV, 401 eV, and 1838 eV, respectively. The carbon and nitrogen regions show sharply defined π^* and σ^* preionization edges which are characteristic of sp^2 hybridization of the graphitelike structure. For the carbon K edge, the π^* fine feature (288 eV) that shifts to the higher energy than that of graphite (284 eV), is suggested to bonding with N or Si atoms. For the nitrogen K edge, the observed 401 eV π^* peak is consistent with the energy of the predicted peak (401–403 eV) that corresponds to the replacement of carbon by the trivalent nitrogen in a hexagonal lattice,²⁶ revealing the bonding structure of N atoms in an SiCN nanotube network. Notably, the double-peaked σ^* feature was observed; it was also observed on the hexagonal BN (Ref. 27) and CN_x .²⁸ Further study is required. Quantification of the EELS spectrum reveals silicon–carbon–nitrogen in the atomic ratios between 5: 80: 15 and 12: 63: 25. The chemical compositions can be varied from tube to tube. The SiCN nanotube network is assumed to have the graphitelike structure. The overall nanotube structures heavily depend on the Si and N concentration; higher Si and N contents yield more corrugated graphitic tubes.

TEM images reveal the bamboo-shaped tubes of many variously sized compartments. Furthermore, the corresponding electron diffraction pattern and HRTEM images confirm the tubes belong to a graphitelike structure (Fig. 5). The zoom-in image shows local graphitization [Fig. 5(b)]. Other regions including the highly defective, and disrupted layers are also observed. The spacing between the two layers is 0.35–0.37 nm larger than that between layers of pure CNT,

0.34 nm. The increased layer spacing is considered to be caused by the introduction of N and Si atoms into the CNT structure, possibly causing distortion; a change in the bonding in pentagonal, heptagonal, or other crystal lattices, and a promotion of bending stress. The graphitic layers are thus distorted by forming bamboo-shaped tubes.

In conclusion, catalyst-assisted SiCN crystals and SiCN nanotubes were synthesized without and with introducing H_2 gas into the precursor gaseous source. Adding Si atoms in the CN network is believed to be an interesting subject for further study. The differences between the nanotubes and the bulk films have opened up many scientific and technological possibilities.

The authors would like to thank the National Science Council (Contract Nos. NSC90-2216-E-009-034, -035, and -040) and the Ministry of Education of Taiwan (Contract No.: 89-E-FA06-1-4) for financially supporting this research.

- ¹A. Y. Liu and M. L. Cohen, *Science* **245**, 841 (1989).
- ²H. L. Chang and C. T. Kuo, *Diamond Relat. Mater.* **10**, 1910 (2001).
- ³H. L. Chang and C. T. Kuo, *Jpn. J. Appl. Phys., Part 1* **40**, 7018 (2001).
- ⁴H. L. Chang and C. T. Kuo, *Mater. Chem. Phys.* **72**, 236 (2001).
- ⁵A. Badzian, T. Badzian, R. Roy, and W. Drawl, *Thin Solid Films* **355**, 417 (1999).
- ⁶L. C. Chen, C. K. Chen, S. L. Wei, D. M. Bhusari, K. H. Chen, Y. F. Chen, Y. C. Jong, and Y. S. Huang, *Appl. Phys. Lett.* **72**, 2463 (1998).
- ⁷H. W. Kroto, J. R. Health, S. C. Öbrien, R. F. Curl, and R. E. Smalley, *Nature (London)* **318**, 162 (1985).
- ⁸S. Iijima, *Nature (London)* **354**, 56 (1991).
- ⁹R. C. Haddon, A. F. Hebard, M. J. Posseinsky, D. W. Murhy, S. J. Duclos, K. B. Lyons, B. Miller, J. M. Rosamilia, R. M. Fleming, A. R. Kortan, S. H. Glarum, A. V. Makhija, A. J. Müller, R. H. Eick, S. M. Zahurak, R. Tycko, G. Dabbagh, and F. A. Thiel, *Nature (London)* **350**, 320 (1991).
- ¹⁰H. Dai, J. H. Hafner, A. G. Rinzler, D. T. Rinzler, D. T. Colbert, and R. E. Smalley, *Nature (London)* **384**, 147 (1996).
- ¹¹G. Che, B. B. Lakshmi, E. R. Fisher, and C. R. Martin, *Nature (London)* **393**, 346 (1998).
- ¹²C. Journet, W. K. Maser, P. Bernier, A. Loiseau, M. Lamy de la Chapelle, S. Lefrant, P. Deniered, R. Lee, and J. E. Fischer, *Nature (London)* **308**, 756 (1997).
- ¹³Q. H. Wang, A. A. Setlur, J. M. Lauerhaas, J. Y. Dai, E. W. Seelig, and R. P. H. Chang, *Appl. Phys. Lett.* **72**, 22 (1998).
- ¹⁴R. Tenne, L. Margulis, M. Genut, and G. Hodes, *Nature (London)* **360**, 444 (1992).
- ¹⁵M. Remskar, Z. Skraba, F. Cleton, R. Sanjines, and F. Levy, *Appl. Phys. Lett.* **69**, 351 (1996).
- ¹⁶N. G. Chopra, R. J. Luyken, K. Cherrey, V. H. Gespi, M. L. Cohen, S. G. Loute, and A. Zettl, *Science* **269**, 966 (1995).
- ¹⁷P. M. Ajayan, O. Stephan, P. Reslich, and C. Colliex, *Nature (London)* **375**, 564 (1995).
- ¹⁸E. G. Wang, *Adv. Mater.* **11**, 1129 (1999).
- ¹⁹J. L. Zimmerman, R. Williams, V. N. Khabashesku, and J. L. Margrave, *Nano Lett.* **1**, 731 (2001).
- ²⁰M. S. Kim, N. M. Rodriguez, and R. T. K. Baker, *J. Catal.* **131**, 60 (1991).
- ²¹M. S. Dresslhaus, G. Dresslhaus, and P. Avouris, *Carbon Nanotube* (Springer, New York, 2001), p. 65.
- ²²R. T. K. Baker, M. A. Barber, P. S. Harris, F. S. Feates, and R. J. Waite, *J. Catal.* **26**, 51 (1972).
- ²³A. Oberlin, M. Endo, and T. Koyama, *J. Cryst. Growth* **32**, 335 (1976).
- ²⁴G. G. Tibbets, *J. Cryst. Growth* **66**, 632 (1984).
- ²⁵R. S. Wagner and W. C. Ellis, *Appl. Phys. Lett.* **4**, 89 (1964).
- ²⁶J. Casanovas, J. M. Ricart, J. Rubio, F. Illas, and J. M. Jimenez-Mateos, *J. Am. Chem. Soc.* **118**, 8071 (1996).
- ²⁷M. Wöbbel, H. Kohl, and P. Kohler-Redlich, *Phys. Rev. B* **59**, 11739 (1999).
- ²⁸W. Q. Han, P. Kohler-Redlich, T. Seeger, F. Ernst, M. Rühle, N. Grobert, W. K. Hsu, B. H. Chang, Y. Q. Zhu, H. W. Kroto, M. Terrones, and H. Terrones, *Appl. Phys. Lett.* **77**, 1807 (2000).